

Article

Nanostructured Lipid Carriers as Promising Delivery Systems for Plant Extracts: The Case of Silymarin

Vieri Piazzini ¹, Beatrice Lemmi ¹, Mario D'Ambrosio ², Lorenzo Cinci ², Cristina Luceri ² , Anna Rita Bilia ¹ and Maria Camilla Bergonzi ^{1,*}

¹ Department of Chemistry, University of Florence, Via U. Schiff 6, 50019 Sesto Fiorentino, Florence, Italy; vieri.piazzini@unifi.it (V.P.); beatrice.lemmi@stud.unifi.it (B.L.); ar.bilia@unifi.it (A.R.B.)

² NEUROFARBA, Department of Neurosciences, Psychology, Drug Research and Child Health, Section of pharmacology and Toxicology, University of Florence, Viale Pieraccini 6, 50139 Florence, Italy; mario.dambrosio@unifi.it (M.D.); lorenzo.cinci@unifi.it (L.C.); cristina.luceri@unifi.it (C.L.)

* Correspondence: mc.bergonzi@unifi.it; Tel.: +39-055-457-3678

Received: 29 June 2018; Accepted: 16 July 2018; Published: 18 July 2018



Featured Application: Silymarin, a standardized extract derived from seeds and fruits of *Silybum marianum* L. Gaertn., is widely used for treatment of various acute and chronic liver toxicities, inflammation, fibrosis and oxidative stress. The extract has low toxicity and exerts significant anti-carcinogenic and anti-inflammatory effects. Recently, it has been reported that the extract is beneficial in type 2 diabetes patients. However, Silymarin is a low water soluble and low permeable compound, belonging to biopharmaceutical class IV type that faces stipulated requirements in delivery design. Thus, to overcome these limitations, the extract was encapsulated into nanostructured lipid carriers. The lipid nanocarriers offer potential applications as natural, low cost and innovative delivery systems to improve solubility, permeability and stability of extract. Other advantages are: possibility of controlled drug release and drug targeting, no biotoxicity of the carrier, biodegradation and no problems with respect to scale-up production in the food and pharmaceutical fields.

Abstract: Background: Silymarin is the extract from seeds of *Silybum marianum* L. Gaertn. and it has been used for decades as hepatoprotectant. Recently, it has been proposed to be beneficial in type 2 diabetes patients. However, silymarin is a poorly water soluble drug with limited oral bioavailability. In this study, nanostructured lipid carriers were proposed to enhance its solubility and intestinal absorption. Methods: Nanostructured lipid carriers were made of Stearic acid:Capryol 90 as lipid mixtures and Brij S20 as surfactant. Formulations were physically and chemically characterized. Stability and in vitro release studies were also assessed. In vitro permeability and Caco-2 cellular uptake mechanism were investigated. Results: Obtained results were based on size, homogeneity, ζ -potential and EE%. Nanostructured lipid carriers could be orally administered. No degradation phenomena were observed in simulated gastrointestinal fluids. Storage stability of suspensions and lyophilized products was also tested. Glucose was selected as best cryoprotectant agent. About 60% of silymarin was released in 24 h in phosphate buffered saline. In vitro parallel artificial membrane permeability assay experiments revealed that the nanocarrier enhanced the permeation of Silymarin. Caco-2 study performed with fluorescent nanoparticles revealed the ability of carrier to enhance the permeation of a lipophilic probe. Cellular uptake studies indicated that active process is involved in the internalization of the formulation. Conclusions: The optimized nanostructured lipid carriers showed excellent chemical and physical stability and enhanced the absorption of silymarin.

Keywords: *Silybum marianum* L. Gaertn.; NLCs; stability; in vitro release; PAMPA; Caco-2; up-take

1. Introduction

A successful drug carrier system should have optimal drug loading and release properties, a long shelf life, and exert a much higher therapeutic efficacy as well as lower side effects. Drug delivery systems are also able to solve several drug problems, including overcoming multi-drug-resistance phenomenon, penetrating cellular barriers that may limit the intended target site, and improving in vivo efficacy of the hydrophilic and lipophilic drugs [1–3]. Therefore, nanotechnology could modulate both drug pharmacokinetics and biodistribution, decreasing potential side effects. In this context, liposomes are the versatile delivery systems formed by the colloidal association of amphiphilic lipid substances which are suitable for delivering both hydrophilic and hydrophobic drugs. Recently, an eco-friendly technology with supercritical fluids for the preparation of nanostructured liposomes was reported as a green alternative in the scale-up because conventional processes require large amounts of organic solvents [4]. Liposome-based formulations also represent a good success for dye delivery, as reported for example in the case of indocyanine green, an FDA-approved fluorescent dye, utilized in various biomedical applications such as drug delivery, imaging, and diagnosis [5]. Liposomes are also advantageous for encapsulating inorganic structures [6,7].

Recently, the use of herbal medicines has increased due to their therapeutic effects and fewer adverse effects as compared to modern medicines. However, many herbal extracts show poor in-vivo activity due to their low solubility, resulting in poor absorption and hence poor bioavailability. Furthermore, there is a great possibility that many compounds of the extract will be destroyed partially or entirely after oral administration. Other components might be metabolized by the liver before reaching the blood circulation.

Novel drug delivery systems represent a valid tool for enhancing bioavailability of herbal drugs. The novel formulations are reported to have remarkable advantages over conventional formulations of plant actives and extracts which include increase of solubility, bioavailability, protection from toxicity, enhancement of pharmacological activity and intracellular uptake, modification of pharmacokinetics and bio-distribution, improved tissue macrophages distribution, sustained delivery and protection from physical and chemical degradation. Furthermore, plant extracts present critical issues due to the wide variety of the compounds contained therein. There are numerous examples of application of the drug delivery systems in this field related to isolated products or herbal extracts [8–13]. In particular, oral absorption of lipophilic extract can be significantly improved using lipid-based non-particulate drug delivery systems, which avoid the dissolution step.

Lipid-based nanocarriers, such as micro- and nanoemulsions, solid-lipid nanoparticles, and nanostructured lipid carriers, represent successful examples of nanoformulations applied to overcome the limitations of natural compounds [14–16]. They can ameliorate solubility, stability, permeation and bioavailability. Lipid-based drug delivery systems are composed by lipids that are also absorption enhancers [17,18] and can be developed in small particle sizes ranging from micro- to nanometers [19,20] to increase the absorption in the hydrophilic environment of the gastrointestinal tract.

Among lipid-based delivery systems, nanostructured lipid carriers (NLCs) offer many advantages, such as long-term stability, increased bioavailability of encapsulated active ingredient, possibility to obtain a controlled or targeted release, versatility in encapsulating both lipophilic and hydrophilic drugs, and high efficiency of encapsulation [21]. NLCs combine two features: they are colloidal carriers of submicron size and they are composed of a solid-lipid core consisting of a mixture of solid lipids blended with a liquid lipid to form a nanosized unstructured matrix and an aqueous phase containing a surfactant or a mixture of surfactants. The partially solid nanostructure enhances the stability of entrapped bioactive, enables high loading capacities, and offers sustained release profiles. The lipid matrix is made of biocompatible and biodegradable materials, which decrease the risk of acute or chronic toxicity. All the components are commercially available and/or approved by regulatory agencies [22–25].

Silymarin (SLM) is one of the oldest traditional herbal medicines used to treat different disorders. SLM is mainly composed of four flavonolignan isomers: silybin, isosilybin, silychristine and

silydianin [26,27]. Hepatoprotective effects of SLM have been demonstrated. It is mildly toxic and exerts significant anti-carcinogenic and anti-inflammatory effects. Recently, its beneficial effect in type 2 diabetes patients has been reported and a number of articles demonstrated its ability to decrease both fasting and mean daily glucose, triglycerides and total cholesterol levels [28,29]. Antidiabetic effect of SLM is attributed to inhibition of gluconeogenesis in the liver and decrease of glucose-6 phosphatase activity [30]. However, it is a low water soluble and low permeable biopharmaceutical class IV type compound that faces stipulated requirements in delivery design.

The aim of the study was to investigate the possibility to delivery lipophilic SLM into NLCs for the preparation of oral dosage form. NLCs were characterized in terms of average diameter, polydispersity, ζ -potential, morphology, and physical and chemical stability. The free-drying process was also considered to increase long-term storage stability of the formulation.

Storage stability and in simulated gastrointestinal conditions was also assessed. SLM in vitro release was studied in different pH media. The release results were applied to define the kinetic and mechanism of SLM release from the NLCs.

The ability of NLCs to ameliorate the permeability of SLM was evaluated in vitro by using parallel artificial membrane permeability assay (PAMPA). Fluorescent nanoparticles were also prepared to verify the capacity of NLCs to enhance the permeability across Caco-2 cells layer. Preliminary cytotoxicity studies were conducted to confirm the optimized biopharmaceutical properties of the lipid carrier. The data obtained from the in vitro tests were compared to elucidate the permeation/absorption mechanism of SLM, which further could be correlated to in vivo behavior. Caco-2 cellular uptake, with or without endocytic inhibitors, was also evaluated, to identify the possible mechanisms of the internalization pathway of the developed NLCs.

2. Materials and Methods

2.1. Materials

Stearic acid, Brij S20, Fluorescein isothiocyanate (FITC, purity $\geq 90\%$, HPLC), Silymarin (SLM), Silibin (Sb, purity $\geq 98\%$, HPLC), Sodium chloride (NaCl), Lipase from porcine pancreas, Pepsin from porcine gastric mucose, Bile salts, Sodium Hydroxide (NaOH), Calcium chloride (CaCl_2), Cholesterol, Lecithin, Phosphate buffered saline (PBS) bioperformance certified, Mucin from porcine stomach, Sodium azide, Chlorpromazine, Indomethacin, DL- α -Tocopherol acetate (Vitamin E), D-Mannitol, D(+)-Glucose anhydrous, Acetone high performance liquid chromatography (HPLC) grade, Acetonitrile HPLC grade, Methanol HPLC grade, Dimethyl sulfoxide (DMSO) HPLC grade, Formic acid analytical grade, Hydrochloric acid (HCl) analytical grade, and 1,7-octadiene 98%, Dichloromethane (CH_2Cl_2) were purchased from Sigma-Aldrich (Milan, Italy). Capryol 90, Lauroglycol 90, Labrafac PG, Labrafac WL 1349, Labrafil M 1944 CS, and Precirol ATO 5 were a gift of Gattefossé (Saint Priest, France). Oleic acid was purchased from Carlo Erba Spa (Milan, Italy). Hemp oil and borage oil were from Galeno srl (Comeana, Prato, Italy). Water was purified by a Milli-Q_{plus} system from Millipore (Milford, CT, USA). Phosphotungstic acid (PTA) was from Electron Microscopy Sciences (Hatfield, PA, USA). The 96-well Multi-Screen PAMPA filter plates (pore size 0.45 μm) were purchased from Millipore Corporation (Tullagreen, Carrigtwohill, County Cork, Ireland). Dialysis kit was from Spectrum Laboratories, Inc. (Breda, The Netherlands).

2.2. Screening of Liquid Lipids

The ability of different liquid lipids (oils) to solubilize SLM was evaluated in order to increase the encapsulation efficiency the NLCs [18]. The solubility of SLM was determined by adding an excess amount of SLM into an exact volume of each selected vehicle while keeping at 500 rpm for 24 h at room temperature. Further the samples were centrifuged at 14,000 rpm for 10 min. The supernatants were diluted with methanol or with methanol/dichloromethane (3:2 *v/v* or 1:1 *v/v*) mixture and finally analyzed with HPLC consisting of an HP 1100 Liquid Chromatograph with a diode-array-detector

(DAD) and controlled with a HP 9000 workstation (Agilent Technologies, Santa Clara, CA, USA). A RP-C18 Luna Omega Polar (150 mm × 3 mm, 5 μm) (Agilent Technologies) analytical column was used. The mobile phases were: (A) formic acid/water pH 3.2; (B) acetonitrile; and (C) methanol with 0.4 mL/min flow rate. The multi-step linear solvent gradient applied was: 0–2 min 10% B and 10% C; 2–6 min 15% B and 22% C; 6–11 min 20% B and 30% C; 11–16 min 30% B and 40% C; 16–18 min 30% B and 40% C; 18–20 min 40% B and 40% C; 20–23 min 40% B and 40% C; 23–27 min 10% B and 10% C; equilibration time 8 min; oven temperature 25 °C. The chromatograms were registered at a wavelength of 288 nm. The calibration curve was prepared using standard silibinin, dissolved in methanol from a concentration range of 0.001–0.100 μg/μL.

2.3. Preparation of NLCs

The NLCs were prepared by the emulsion–evaporation method at high temperature and solidification at low temperature [31]. The lipid phase, composed of Stearic Acid (80 mg, solid lipid) and Capryol 90 (20 mg, liquid lipid) was dissolved into 5 mL of acetone and heated under magnetic stirring. The resulted organic solution was added dropwise into the aqueous phase containing Brij S20 (200 mg in 30 mL) at 1000 rpm and 75 °C to induce the acetone evaporation. Further, the concentrated emulsion was quickly added into an equal volume of cold distilled water in an ice bath under fast stirring at 1000 rpm for 1 h to induce NLCs formation. The obtained NLCs were harvested and stored at 4 °C. The final concentrations of stearic acid, Capryol 90 and Brij S20 were 0.57% *w/v*, 0.14% *w/v* and 1.43% *w/v*, respectively.

2.4. Preparation of SLM-Loaded NLCs and FITC-Loaded NLCs

The SLM-loaded NLCs (SLM-NLCs) and the fluorescent NLCs (FITC-NLCs) were prepared according to the method previously described [31]. Fluorescein isothiocyanate (FITC) ($\lambda_{ex} = 492$ nm, $\lambda_{em} = 518$ nm, green) or SLM were added to lipid phase to obtain a final concentration of 0.04% *w/v* for FITC and 0.29% *w/v* for SLM. Further the formulations were hermetically sealed and stored at 4 °C, protected from light. In addition, the SLM-NLCs sample was divided into three parts: one of these was frozen with liquid nitrogen and then moved to the freeze-drier [32]. The other two were freeze dried after the addition of D-Glucose anhydrous (10% *w/v*) or D-Mannitol (10% *w/v*) as cryoprotective agents. The drying time was 24 h. The reaction yields were calculated as the weight percentage of freeze-dried formulations, with respect to the total weight of the substances used for the preparation.

2.5. Particle Size, Polydispersity Index and ζ -Potential

The evaluation of the particle size and the polydispersity index (PDI) was performed by dynamic light scattering using a Zsizer Nanoseries ZS90 (Malvern Instrument, Worcestershire, UK) at a fixed angle of 90° and at 25 °C. The ζ -potential, indicating the electric charge on the NLCs surface and the physical stability of the formulations, was calculated using the Helmholtz–Smoluchowsky equation using the same instrument. To avoid multiple scatterings of the light, for all measurements, samples were diluted to suitable concentration with distilled water. The analyses were performed in triplicate.

2.6. Transmission Electron Microscopy

The shape and the surface structure of NLCs were investigated by transmission electron microscope (TEM, Jeol 1010, Tokyo, Japan). The samples were opportunely diluted with distilled water, then were dropped on a 200 mesh carbon film-covered copper grid and negatively stained with phosphotungstic acid aqueous solution (1% *w/v*). After drying, the grid containing the sample was observed with the TEM [14].

2.7. Determination of Encapsulation Efficiency and Recovery

Dialysis bag method was applied to remove free SLM (or FITC) from the formulations. The bag was inserted for 1 h in 1 L of distilled water, with the aim to determine the encapsulation efficiency of the NLCs. Then, the sample was diluted (1:10 *v/v*) with methanol and sonicated in an ultrasonic bath for 30 min to extract SLM (or FITC). The resulted mixture was centrifuged for 10 min at 14,000 rpm and analyzed by HPLC [33]. FITC analyses were performed on the same apparatus, with the column used for SLM. The eluents were: (A) formic acid/water pH 3.2; and (B) acetonitrile. The gradient applied was: 0–2 min 20% B; 2–22 min 20–85% B; 22–25 min 85–100% B; 25–28 min 20% B; equilibration time 7 min; temperature 25 °C; flow rate 0.4 mL/min. In this case, the chromatograms were acquired at 224 nm. The linearity range of responses of Sb and FITC dissolved in CH₃OH was determined on five concentration levels from 0.001 µg/µL to 0.054 µg/µL.

The encapsulation efficiency was calculated by the following Equation (1):

$$\text{Encapsulation efficiency} = \frac{\text{SLM (or FITC) encapsulated}}{\text{Total SLM (or FITC)}} \times 100 \quad (1)$$

The recovery was estimated following the same procedure but without dialysis purification and was calculated by using the following Equation (2):

$$\text{Recovery} = \frac{\text{SLM (or FITC) detected}}{\text{Total SLM (or FITC)}} \times 100 \quad (2)$$

2.8. Stability Studies

2.8.1. Storage Stability

Stability studies on particle size, PDI, ζ-potential and encapsulation efficiency of SLM-NLCs as suspension at 4 °C and freeze-dried SLM-NLCs stored at room temperature were conducted at Days 0, 10, 20 and 30 from the production by light scattering and HPLC analyses. Phase separation and turbidity were also investigated in the case of the suspension, while the freeze-dried NLCs were evaluated for the appearance of the powder and for the redispersibility time.

2.8.2. Stability in Simulated Gastrointestinal Conditions

The NLCs sample was incubated in an equal volume of simulated gastric fluid (SGF) for 2 h at 37 °C and subsequently in simulated intestinal fluid (SIF) for further 2 h at 37 °C. SGF was prepared dissolving pepsin (0.32% *w/v*), 2 g of sodium chloride and 7 mL of HCl in 1 L of distilled water. The pH of the solution was adjusted to 2.0 with HCl 1 M. The composition of SIF was: lipase (0.04% *w/v*), bile salts (0.07% *w/v*), pancreatin (0.05% *w/v*) and calcium chloride 750 mM. The pH was adjusted to 7.0 with NaOH. The effect of SGF and SIM on physical properties of NLCs was evaluated by measuring particle size and PDI.

2.9. In Vitro Release

In vitro release of SLM from NLCs was investigated using the dialysis bag method. Regenerated cellulose membranes with a MWCO of 3–5 kD were used to retain the NLCs and allow the diffusion of SLM into the release medium. Phosphate buffer saline (PBS, pH 7.4), SGF without pepsin and enzyme-free SIF were taken as dissolution medium. Two milliliters of SLM-loaded NLCs were deposited into the dialysis membrane and placed in 200 mL of release medium at 37 °C with stirring at 150 rpm. At definite time intervals up to 24 h, 1 mL was withdrawn and replaced with fresh dissolution medium. SLM released was quantified by HPLC.

For evaluating the kinetic and mechanism of drug release from the liposomes, Korsmeyer–Peppas model, Hixson–Crowell model, Higuchi model, and first- and zero-order mathematical models were

used and best fitted model was selected based on high regression coefficient (R^2) value for the release data.

2.10. PAMPA Experiments

The permeation of SLM alone and SLM-NLCs through artificial membranes was determined using the protocol optimized in our previous studies [10,15,16,34]. The 96-well microtiter PVDF filter plate was impregnated with 10 μ L of a lecithin (1% *w/v*) and cholesterol (0.8% *w/v*) in 1,7-octadiene solution. Then, the donor plate was filled with 250 μ L of SLM solution or SLM-NLCs and placed upon the acceptor plate containing 250 μ L of 5% *v/v* DMSO in PBS. The plate assembly was placed into a sealed container to prevent evaporation and incubated at room temperature for 4 h. After the incubation, the samples were diluted with methanol, sonicated in an ultrasonic bath for 30 min and centrifuged for 10 min at 14,000 rpm for HPLC analyses. The permeability of SLM and the recovery value were calculated according to Equations (3)–(5) reported in the literature [35,36]:

$$P_e = C \times -\ln\left(1 - \frac{[\text{Compound}]_A}{[\text{Compound}]_{eq}}\right); \text{ where } C = \frac{V_D \times V_A}{(V_D + V_A) \times A \times t}; \quad (3)$$

$$[\text{Compound}]_{eq} = \frac{[\text{Compound}]_D \times V_D + [\text{Compound}]_A \times V_A}{(V_D + V_A)} \quad (4)$$

$$\text{Recovery (\%)} = \frac{[\text{Compound}]_D \times V_D + [\text{Compound}]_A \times V_A}{([\text{Compound}]_{D_0} \times V_D)} \times 100 \quad (5)$$

where P_e is the effective permeability (cm/s); A is the effective filter area (cm²); V_D and V_A are the volumes in the acceptor and the donor plates (mL), respectively; t is incubation time (s); $[\text{Compound}]_A$ and $[\text{Compound}]_D$ are the concentrations of SLM in the acceptor and the donor plates at time t , respectively; and $[\text{Compound}]_{D_0}$ is the concentration of SLM in the donor plate at time 0.

2.11. Caco-2 Cell Culture Experiments

2.11.1. Cell Lines

The colorectal adenocarcinoma cell line Caco-2 was purchased from American Tissue Type Culture Collection (Manassas, VA, USA) and cultured in Dulbecco's modified Eagle's medium (Thermo Fisher Scientific, Rodano, Milan, Italy) with 20% fetal bovine serum (FBS) (Thermo Fisher Scientific, Rodano, Milan, Italy), 100 U/mL penicillin-streptomycin (Thermo Fisher Scientific, Rodano, Milan, Italy) in 5% CO₂ at 37 °C.

2.11.2. Cell Culture Experiments

An MTS assay was used to determine the cell viability after exposure to NLCs for 2 h, as previously described [37]. The relative cell viability was expressed as a percentage of the untreated control group.

2.11.3. Transport Studies

For the permeation studies, Caco-2 cells were seeded into 12-well PET transwell plates (1.13 cm² growth surface area and pore size 0.4 μ m, Greiner Bio-One, Milan, Italy) at a density of 2×10^4 cells/cm² and grown for 21 days to form a confluent monolayer. The integrity of the cellular barrier was assessed using Lucifer Yellow permeability test [16]. Samples of media were collected from the basal compartment of each transwell plate and replaced with fresh HBSS at 0 (before sample addition), 30 and 60 min. The FITC concentrations of these samples were determined by HPLC and adjusted to reflect the change in volume at each successive sampling point. LY measurements were also taken at the end of the experiment.

2.11.4. Uptake Studies

To identify the transepithelial transport mechanism, Caco-2 cells were pre-incubated with sodium azide (an ATP synthesis inhibitor, 1 μ M), chlorpromazine (a clathrin blocker, 15 μ M), and indomethacin (a caveolin-dependent endocytosis inhibitor, 25 μ M) for 30 min followed by addition of NLCs 1:180 for 1 h, or maintained at 4 °C during the NLCs exposure. At the end of the treatments, the amount of FITC was measured on cellular lysate by HPLC analysis. In parallel, Caco-2 cells, grown on histological slides, were treated in the same condition, fixed in 4% formaldehyde in 0.1 mol/L phosphate buffer, pH 7.4, for 10 min and observed by fluorescence microscopy (Labophot-2 Nikon, Tokyo, Japan). Ten photomicrographs were randomly taken for each sample and fluorescence was measured using ImageJ 1.33 image analysis software (<http://rsb.info.nih.gov/ij>).

3. Results and Discussion

3.1. NLCs Preparation and Characterization

The selection of the components for NLCs preparation is important to obtain good stability of the formulation and high encapsulation efficiency of the extract. For this purpose, solubility studies of SLM in different liquid lipids (Table 1) have been performed. The selected excipients are approved and recognized as safe substance, as the purpose of this study is to produce formulations suitable for oral administration.

Table 1. Solubility of silymarin (SLM) in different liquid lipids/oils. Results are expressed as means \pm standard deviation, $n = 3$.

Liquid Lipid	SLM Solubility (mg/mL)
Borage oil	0.12 \pm 0.01
Capryol 90	13.80 \pm 0.14
Hemp oil	0.13 \pm 0.01
Labrafac PG	0.77 \pm 0.01
Labrafac WL 1349	0.72 \pm 0.09
Labrafil M 1994	2.10 \pm 0.15
Lauroglycol 90	10.00 \pm 0.01
Oleic acid	-
Vitamin E	0.53 \pm 0.15

As evidenced in Table 1, the solubility of SLM in the various analyzed liquid lipids is always greater than in water (0.26 mg/mL), except in the case of borage and hemp oil. The best result was obtained using Capryol 90 (13.80 mg/mL) and Lauroglycol (10.00 mg/mL).

Capryol 90 is a colorless liquid with HLB of 5, consisting of mono propylene glycol/esterified with caprylic acid and used for oral, topical, rectal and vaginal formulations. Lauroglycol 90 is an oil with HLB equal to 3, consisting of mono/di-esterified propylene glycol with lauric acid and used as an excipient for topical and oral pharmaceutical formulations.

The choice of lipids and surfactants used for NLCs formulation was performed by evaluating not only the solubility of SLM, but also the HLB of oils and tensides, with the aim to obtain good encapsulation efficacy and high stability of the carriers. Stearic acid and Precirol ATO were tested as solid lipids, Capryol and Lauroglycol as liquid lipids. Among the surfactants, selected hydrophilic compounds were Tween 80 (HLB 15), Tween 20 (HLB 16.7) and Brij S20 (HLB 15). These tensides were chosen based on the HLB value and solubilizing capacities.

Different ratios of solid and liquid lipids and tensides were evaluated. Some tested formulations showed good physical requires for oral administration, such as size and PDI, but they were not stable. Finally, the optimized NLCs are reported in Table 2. Its composition was Stearic acid/ Brij S20 (1:2 w/w) and Capryol 90 (2:8 w/w respect to solid lipid). Brij S20 is a non-ionic tenside, derived from stearic acid covalently grafted with PEG 1000, which form a hydrophilic steric barrier around the NLCs

and increase their stability [14]. This selected formulation was able to load 40 mg/mL of extract (SLM-NLCs), with an EE% of 92.4%. The presence of SLM does not influence the stability of the NLCs: when SLM were loaded into the nanoparticles, the formulation showed the same physical parameters than empty NLCs. TEM micrographs provided information on morphology and dimensions of nanoparticles: the formulation had a spherical structure with a diameter like that obtained through DLS analyses (Figure 1).

FITC, a lipophilic fluorescent dye, was incorporated into NLCs as a probe to perform in vitro studies with Caco-2 cells and to elucidate trans-endothelial transport. Fluorescent NLCs were prepared as reported for empty NLCs, by adding FITC to the lipid phase (FITC-NLCs). Their physical and chemical parameters are shown in Table 2. All formulations are useful for oral administration.

The high ζ -potential confirms their stability, as also supported by colloidal stability data.

Furthermore, the method applied for the preparation of the NLCs allows avoiding the degradation of the loaded extract or probe, as evidenced by the high recovery values (Table 2).

Table 2. Physical and chemical properties of empty NLCs, SLM-NLCs and Fluorescein isothiocyanate-NLCs (FITC-NLCs). Results are expressed as means \pm standard deviation, $n = 3$.

Sample	Particle Size (nm)	Polydispersity Index (PDI)	ζ -Potential (mV)	EE (%)	Recovery (%)
NLCs	194.5 \pm 3.7	0.24 \pm 0.02	-36.0 \pm 0.9	-	-
SLM-NLCs	213.6 \pm 16.0	0.17 \pm 0.04	-31.6 \pm 0.5	92.4 \pm 4.1	94.8 \pm 1.8
FITC-NLCs	215.0 \pm 0.3	0.24 \pm 0.01	-37.4 \pm 0.9	95.7 \pm 1.2	98.5 \pm 0.5

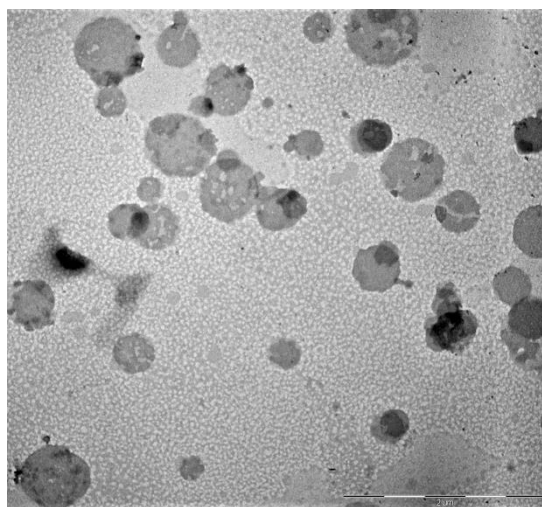


Figure 1. Transmission Electron Microscope (TEM) images of Silymarin (SLM)-NLCs.

Then, the SLM-NLCs were freeze-dried in the presence of a cryoprotectant, both to prolong its physical and chemical stability over time, and to reduce microbial contamination. From the literature, different cryoprotectants, are reported, such as glucose, maltose, trehalose, sucrose, mannitol and lactose, from 5 to 20% w/v [38]. Glucose (10% w/v) and mannitol (10% w/v) were tested for the NLCs (Table 3).

A sample of SLM-NLCs was lyophilized without cryoprotectant, while two other samples in the presence of glucose and mannitol, respectively. The dispersions were physically characterized with DLS after resuspension with water. The results (Table 3) highlighted a significant increase in size and PDI values in the absence of cryoprotectant. On the contrary, the lyophilization with glucose allowed preserving the stability of the system providing nanoparticles with almost identical dimensions and homogeneity those detected before the freeze-drying process. Finally, the nanoparticles lyophilized with mannitol revealed a certain increase in terms of average diameter and inhomogeneity.

Table 3. Physicochemical characterization and reaction yields of SLM-NLCs after freeze-drying process. Light Scattering and High performance liquid chromatography (HPLC) analyses were performed after reconstitutions of the samples in water. Results are expressed as means \pm standard deviation, $n = 3$.

Freeze-Dried Product	Particle Size (nm)	PDI	ζ -Potential (mV)	EE (%)	Yield (%)
SLM-NLCs	383.6 \pm 4.7	0.32 \pm 0.03	−30.1 \pm 0.8	64.1 \pm 0.2	97.8 \pm 0.1
SLM-NLCs + Glucose	205.2 \pm 2.7	0.16 \pm 0.04	−36.7 \pm 0.5	87.6 \pm 4.9	98.9 \pm 0.2
SLM-NLCs + Mannitol	305.1 \pm 9.5	0.24 \pm 0.01	−32.6 \pm 0.7	76.0 \pm 3.1	99.2 \pm 0.1

The results confirm the advantage of cryoprotectants in preventing the aggregation of nanoparticles during the lyophilization process. In particular, glucose allows obtaining a freeze-dried product easily re-dispersible, soft and voluminous. In fact, the cryoprotectants interact with the polar portions of surfactants, forming a kind of protective coating. They also reduce the crystallization processes, favoring the amorphous state of the frozen sample [38].

3.2. Chemical and Physical Storage Stability

After four weeks at 4 °C, SLM-NLCs suspensions were chemically and physically stable. No changes in size and homogeneity occurred: dimensions were 200.3 \pm 2.6 nm with PDI of 0.10 \pm 0.03. The ζ -potential was monitored up to 30 days of storage, and no significant evolution was found, with final value of −24.3 \pm 0.7 mV. Furthermore, EE% and recovery% did not decrease during storage (EE% 86.7 \pm 2.4; recovery% 89.3 \pm 1.2). Thus, developed formulations are able to prevent the degradation of incorporated compound. This represents an important result, considering that, in many cases, chemical and physical instabilities were observed when NLCs were stored as aqueous suspension due to lipid crystallization, polymorphic transformations, aggregation phenomena and hydrolysis processes.

Analogous study was performed on freeze-dried products. Both products maintain the same physical characteristics as before freeze-drying (size 216.7 \pm 4.7 nm, PDI 0.34 \pm 0.01 and −35.2 \pm 1.3 mV, in the case of glucose; and size 300.1 \pm 2.1 nm, PDI 0.28 \pm 0.01 and −33.0 \pm 0.1 mV, in the case of mannitol) but there is a small decrease in EE% (79.8 \pm 2.5 for glucose and 73.5 \pm 1.2 for mannitol). Recovery for both formulations is more than 80%.

3.3. Stability in Simulated Gastrointestinal Fluids

NLCs have been formulated not only for increasing bioavailability of the SLM but also to protect the active components from degradation during gastrointestinal transit. The integrity of the nanoparticles can represent an important prerequisite to reach the sites of absorption in the intestine and obtain increased uptake at the intestinal epithelium itself [39]. For this purpose, the physical stability of the formulation in simulated gastrointestinal conditions was determined by subjecting it to simulated gastric digestion at pH 2.0 in presence of pepsin, followed by simulated intestinal digestion in presence of the pancreatin-lipase-bile salts mixture.

After 2 h of incubation in SGF followed by 2 h of incubation in SIF, NLCs resulted stable and no aggregation or degradation phenomena occurred (Table 4). This stability in acidic and intestinal conditions may be due to the effect of steric stabilization of nonionic surfactant, Brij S20, which decreases the flocculation and coalescence phenomena with its molecular structure. In addition, this stability can be conferred also by the properties of lipids, Stearic acid and Capryol 90, able to protect encapsulated SLM by enzymatic degradation and by pH conditions [40].

Table 4. Physical stability of SLM-NLCs in simulated gastrointestinal fluids (SGF: simulated gastric fluid; SIF: simulated intestinal fluid). Results are expressed as means \pm standard deviation of three experiments.

Medium	Size	PDI
SGF	258.4 \pm 3.9	0.34 \pm 0.05
SIF	205.2 \pm 2.8	0.28 \pm 0.10

3.4. In Vitro Release

In vitro release studies were performed in different pH media without enzymes: PBS, SGF (pH 2) and SIF (pH 7). The studies have been conducted to evaluate if and how different pH conditions can influence the release of SLM from the NLCs. The in vitro release profiles are shown in Figure 2. In PBS, the absence of the burst effect is evident: the release of SLM is not immediate but gradual, up to a maximum percentage of 66.3% in the 24 h.

In the gastric environment during the first 2 h, corresponding to transit through the stomach, only the 9.6% of the SLM, was released. Thus, the developed NLCs remain intact in SGF, according to the previous data of the stability study, and they prevent degradation of the encapsulated extract and can be promising carriers for the transport of a large amount of SLM into the intestine.

In simulated intestinal environment, a controlled release of SLM with a maximum of 15.4% released within 24 h was observed. These results suggest that, following the gastrointestinal tract transit, 84.6% of SLM remains encapsulated in NLCs, allowing greater intestinal absorption.

The lower release obtained in simulated gastro-intestinal conditions suggests that the formulation protects SLM from degradation and guarantees a slow release of the extract due to the lipid matrix. NLCs demonstrated promising potential to prevent burst release and degradation of SLM which remained entrapped into nanoparticles and could be absorbed and reach the target site after oral administration [41]. The absence of the burst effect can be justified by the low percentage of liquid lipid which does not lead to the formation of an outer shell containing high concentrations of SLM, but the oil is distributed randomly in the solid lipid matrix [42]. Such a prolonged release can allow increased absorption of the drug, maintaining a constant concentration in the plasma.

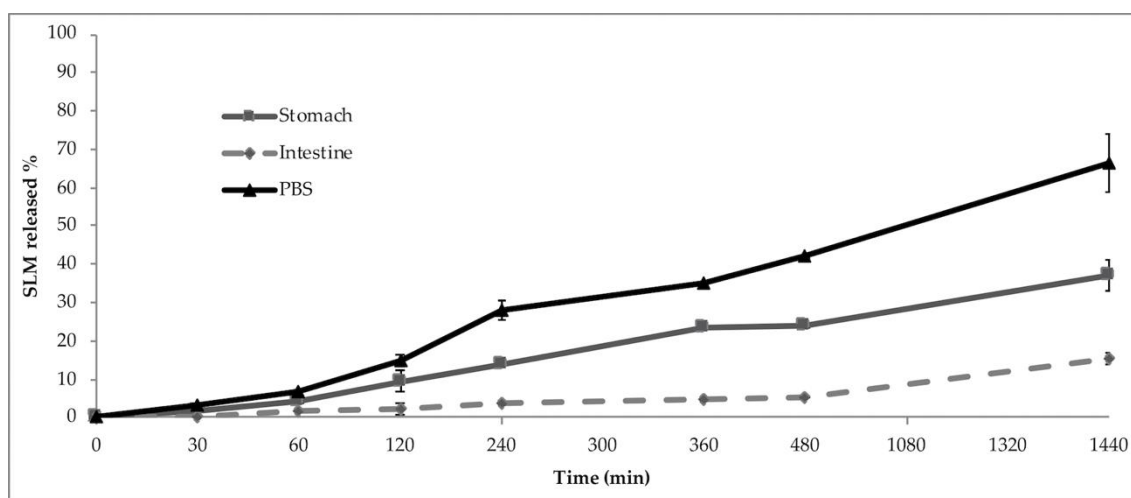


Figure 2. In vitro release studies of SLM-NLCs in phosphate buffered saline (PBS) pH 7.4 (black line) and in simulated gastrointestinal fluids (dark grey line and light grey dotted line). Results are expressed as means \pm standard deviation, $n = 3$.

Different theoretical models were considered to examine the nature of release. Drug release mechanism in PBS was defined by fitting SLM release data during 24 h to various kinetics models. By comparing the regression coefficient values (Zero-order: 0.8263; First-order: 0.9304; Korsmeyer–Peppas: 0.7578; Hixson: 0.8998; Higuchi: 0.9664), the Higuchi model was shown to be the most adequate to describe the kinetics of NLCs. Thus, the diffusion process controlled the release mechanism. Furthermore, if analyzed according to Korsmeyer–Peppas model, the release exponent n was >0.89 , and it confirms that the release follows a super case II drug-transport mechanism and the mechanism can be inferred to follow a non-Fickian diffusion process.

3.5. PAMPA Studies

The PAMPA is an in vitro method used to estimate transcellular passive permeability. It is considered robust, reproducible and fast [43]. The assay could be applied not only in the preformulation studies of single molecules but also for complex matrices such as plant extracts [39] and compounds loaded into formulations, i.e., SLNs and microemulsions [15,16,33,34,44].

Considering that most compounds reach the blood stream by passive mechanism, PAMPA could be a helpful complement to Caco-2 assay to predict the oral absorption of SLM.

The effective permeability (P_e) value after 4 h of incubation was $12.1 \pm 1.4 \times 10^{-6}$ for free SLM and $132 \pm 11 \times 10^{-6}$ in the case of extract loaded NLCs. Passive permeation of SLM was improved considerably with respect to aqueous solution (11-fold higher) when formulated. The recovery was 100% for the SLM-NLCs and 95% for the saturated aqueous solution of SLM. A high recovery value, above 80% is a proof of an acceptable permeation prediction. Moreover, this result suggests that there was neither relevant extract membrane retention nor binding to the surface of the filter. The developed formulations represent a successful attempt to ameliorate passive permeation of SLM.

3.6. Caco-2 Cell Culture Experiments

Permeation studies were performed using a cell-based model in order to complete in vitro characterization of NLCs and understand oral absorption mechanisms. For this aim, Caco-2 cells are considered the most predictive in vitro model to estimate not only passive intestinal diffusion, as previously described for PAMPA, but also active transport processes, paracellular permeability and active efflux [10,15,16].

The cytotoxicity of FITC-NLCs was first investigated by MTS test with the aim to select the most appropriate concentration for transport studies. As shown in Figure 3, NLCs exerted a quite low cytotoxicity (about 30%) diluted 1:180. This is a good result considering that NLCs undergoes a dilution from 1:200 to 1:1000 when they are oral administered.

Thus, the transport studies were conducted by using this dilution and 1 h as exposition time.

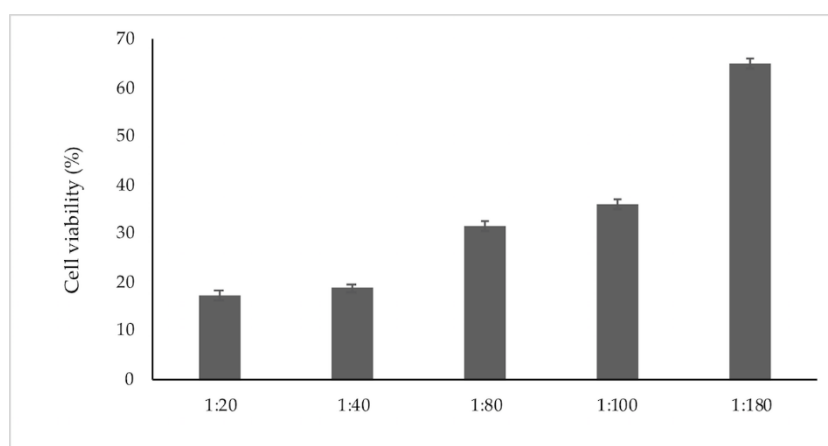


Figure 3. Viability of Caco-2 cells exposed to Fluorescein isothiocyanate-NLCs (FITC-NLCs) (1:20 to 1:180), for 2 h.

P_{app} values are reported in Figure 4; it can be observed that the permeation of FITC, a lipophilic probe not able to cross the Caco-2 monolayer, was improved when formulated into NLCs, reaching an apparent permeability of 102.4×10^{-6} cm/s after 30 min.

To investigate the possible pathways of FITC-NLCs internalization in Caco-2 cells, its uptake was followed in different energetic conditions and in presence of endocytosis inhibitors.

The representative images in Figure 5a showed that the internalization of the FITC-NLCs was significantly reduced when incubated at different energetic conditions (4 °C and ATP-depleted

condition). The experimental results indicated in fact that the cellular uptake of NLCs at 4 °C was only about 37% of that at 37 °C and sodium azide (an energy inhibitor) was also able to reduce, although to a lesser extent, the cellular uptake. At low temperatures, a higher rigidity and a lower permeability of lipid bilayer have been demonstrated and could explain this difference [45].

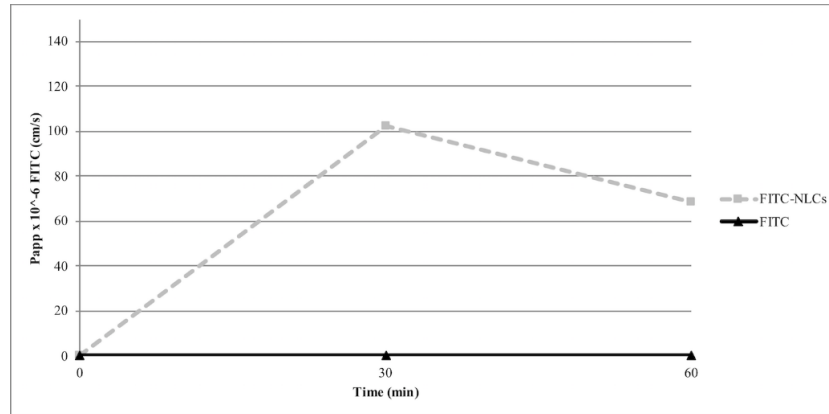


Figure 4. Apparent permeability coefficient (P_{app}) of free FITC or loaded into NLCs (FITC-NLCs) across the Caco-2 monolayer after 1 h of incubation.

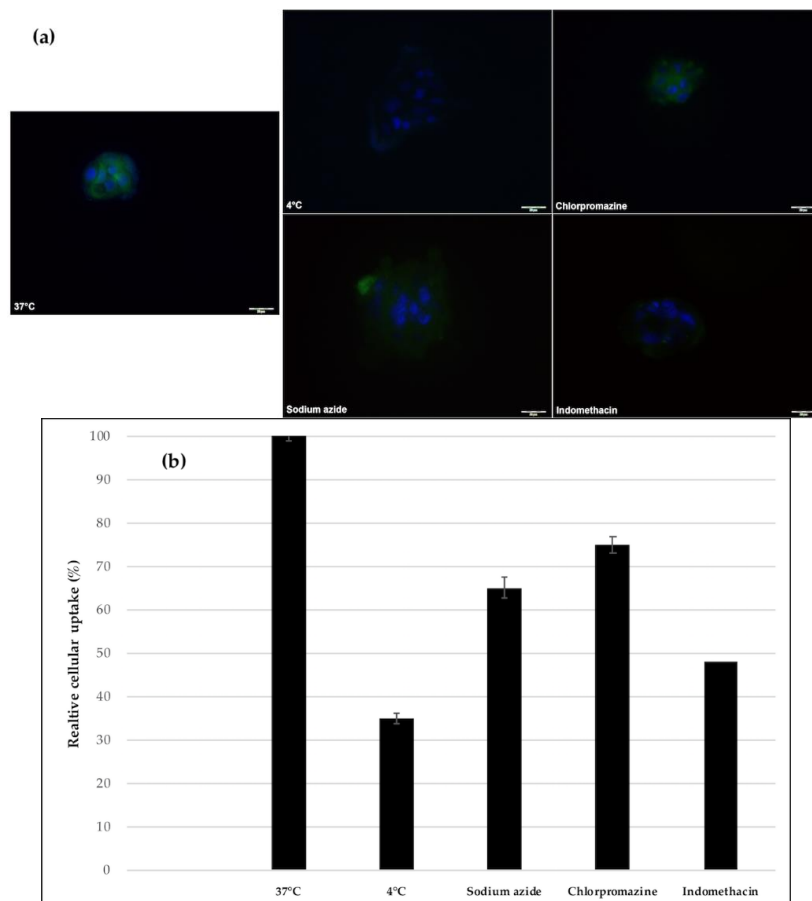


Figure 5. (a) Cellular uptake of FITC-NLCs (green staining), in the presence of endocytic inhibitors. Nuclei were stained with DAPI. Final magnification 400×; scale bar 20 μm. (b) Percentage of intracellular FITC in Caco-2 cells after 1 h of exposure to FITC-NLCs at 37 °C (100%) or in the presence of endocytic inhibitors. Results are expressed as means ± standard deviation, $n = 3$.

The dependency of cellular uptake on energy indicates that the internalization possibly occurs by endocytosis. To further illustrate about the particular internalization pathway involved, Caco-2 cells were pretreated with inhibitors: chlorpromazine blocks clathrin-dependent endocytosis and indomethacin inhibits caveolin-dependent endocytosis. The cellular uptake of FITC-NLCs seems to be a rather complex process not dependent solely on a single mechanism. Our results indicated that they are incorporated into the intestinal epithelia mainly via the caveolin-dependent endocytic pathway, whereas the endocytosis mediated by clathrin was less involved in the uptake, reducing it by about 20% (Figure 5b).

4. Conclusions

These studies confirmed that the developed NLCs offer a promising delivery system for enhancing the solubility and intestinal permeability of lipophilic SLM.

Stearic acid, Capryol and Brij S20 were chosen as solid lipid, liquid lipid and non-ionic surfactant, respectively. Based on obtained results of physical and chemical characterizations, developed formulations could be orally administered. The system showed excellent chemical and physical stability during storage at 4 °C and after incubation into simulated gastrointestinal environment. In vitro release indicated that NLCs may prevent burst release and gastric degradation of SLM. Moreover, the slow release of SLM suggests homogeneous entrapment of the compound throughout the lipid matrix.

Caco-2 cells were selected to form simulative intestinal epithelial cell monolayers to study the permeation and the related transport mechanisms. The results indicated that the formulations were successful in enhancing the permeation of SLM and that the transport of the NLCs across the cell monolayer is energy-dependent and mediated by clathrin- and caveolae (or lipid raft)-related routes.

Author Contributions: Conceptualization, M.C.B., V.P. and C.L.; Methodology, V.P., B.L., L.C. and M.D.; Investigation, V.P., B.L., L.C. and M.D.; Data Curation, V.P., L.C. and M.D.; Writing—Original Draft Preparation, M.C.B., V.P. and C.L.; Writing—Review and Editing, M.C.B., V.P., C.L., and A.R.B.; Supervision, M.C.B. and C.L.; Project Administration, M.C.B.; and Funding Acquisition, M.C.B.

Funding: This research was funded by Ente Cassa di Risparmio di Firenze 2016, grant number 2016.0802.

Acknowledgments: The authors acknowledge Dott.ssa M. Cristina Salvatici Centro di Microscopie Elettroniche “Laura Bonzi”, ICCOM, Consiglio Nazionale delle Ricerche (CNR), Via Madonna del Piano, 10 Firenze, Italy.

Conflicts of Interest: The authors declare no conflict of interest.

References

1. Hans, M.L.; Lowman, A.M. Biodegradable nanoparticles for drug delivery and targeting. *Curr. Opin. Solid State Mater. Sci.* **2002**, *6*, 319–327. [[CrossRef](#)]
2. Jabr-Milane, L.S.; van Vlerken, L.E.; Yadav, S.; Amiji, M.M. Multi-functional nanocarriers to overcome tumor drug resistance. *Cancer Treat. Rev.* **2008**, *34*, 592–602. [[CrossRef](#)] [[PubMed](#)]
3. Kankala, R.K.; Kuthati, Y.; Sie, H.-W.; Shih, H.-Y.; Lue, S.-I.; Kankala, S.; Jeng, C.C.; Deng, J.P.; Weng, C.F.; Liu, C.L.; et al. Multi-laminated metal hydroxide nanocontainers for oral-specific delivery for bioavailability improvement and treatment of inflammatory paw edema in mice. *J. Colloid Interface Sci.* **2015**, *458*, 217–228. [[CrossRef](#)] [[PubMed](#)]
4. Kankala, R.K.; Zhang, Y.S.; Wang, S.B.; Lee, C.H.; Chen, A.-Z. Supercritical Fluid Technology: An Emphasis on Drug Delivery and Related Biomedical Applications. *Adv. Healthc. Mater.* **2017**, *6*, 1700433. [[CrossRef](#)] [[PubMed](#)]
5. Han, Y.-H.; Kankala, R.K.; Wang, S.B.; Chen, A.-Z. Leveraging Engineering of Indocyanine Green-Encapsulated Polymeric Nanocomposites for Biomedical Applications. *Nanomaterials* **2018**, *8*, 360. [[CrossRef](#)] [[PubMed](#)]
6. Kankala, R.K.; Liu, C.G.; Chen, A.Z.; Wang, S.B.; Xu, P.Y.; Mende, L.K.; Liu, C.L.; Lee, C.H.; Hu, Y.F. Overcoming Multidrug Resistance through the Synergistic Effects of Hierarchical pH-Sensitive, ROS-Generating Nanoreactors. *ACS Biomater. Sci. Eng.* **2017**, *3*, 2431–2442. [[CrossRef](#)]

7. Kankala, R.K.; Kuthati, Y.; Liu, C.L.; Mou, C.Y.; Lee, C.H. Killing cancer cells by delivering a nanoreactor for inhibition of catalase and catalytically enhancing intracellular levels of ROS. *RSC Adv.* **2015**, *5*, 86072–86081. [[CrossRef](#)]
8. Devi, K.V.; Nimisha, J.; Valli, K.S. Importance of novel drug delivery systems in herbal medicines. *Pharmacogn. Rev.* **2010**, *4*, 27–31. [[CrossRef](#)] [[PubMed](#)]
9. Li, W.; Yi, S.; Wang, Z.; Chen, S.; Xin, S.; Xie, J.; Zhao, C. Self-nanoemulsifying drug delivery system of persimmon leaf extract: Optimization and bioavailability studies. *Int. J. Pharm.* **2011**, *420*, 161–171. [[CrossRef](#)] [[PubMed](#)]
10. Piazzini, V.; Bigagli, E.; Luceri, C.; Bilia, A.R.; Bergonzi, M.C. Enhanced solubility and permeability of Salicis cortex extract by formulating as Microemulsion. *Planta Med.* **2018**. [[CrossRef](#)] [[PubMed](#)]
11. Bergonzi, M.C.; Isacchi, B.; Antiga, E.; Caproni, M. Curcumin nanoparticles potentiate therapeutic effectiveness of acitretin in moderate-to-severe psoriasis patients and control serum cholesterol levels. *J. Pharm. Pharmacol.* **2018**. [[CrossRef](#)]
12. Bilia, A.R.; Piazzini, V.; Guccione, C.; Risaliti, L.; Asprea, M.; Capecchi, G.; Bergonzi, M.C. Improving on nature: The role of nanomedicine in the development of clinical natural drugs. *Planta Med.* **2017**, *83*, 366–381. [[CrossRef](#)] [[PubMed](#)]
13. Bilia, A.R.; Isacchi, B.; Righeschi, C.; Guccione, C.; Bergonzi, M.C. Flavonoids loaded in nanocarriers: An opportunity to increase oral bioavailability and bioefficacy. *Food Nutr. Sci.* **2014**, *5*, 1212–1227. [[CrossRef](#)]
14. Graverini, G.; Piazzini, V.; Landucci, E.; Casamenti, F.; Pantano, D.; Pellegrini-Giampietro, D.; Bilia, A.R.; Bergonzi, M.C. Preparation of solid lipid nanoparticles for the delivery of Andrographolide across the blood-brain barrier: In vitro and in vivo evaluations. *Colloids Surf. B* **2018**, *161*, 302–313. [[CrossRef](#)] [[PubMed](#)]
15. Piazzini, V.; Rossetti, C.; Bigagli, E.; Luceri, C.; Bilia, A.R.; Bergonzi, M.C. Prediction of permeation and cellular transport of *Silybum marianum* extract formulated in nanoemulsion by using PAMPA and Caco-2 cell models. *Planta Med.* **2017**, *83*, 1184–1193. [[CrossRef](#)] [[PubMed](#)]
16. Piazzini, V.; Monteforte, E.; Luceri, C.; Bigagli, E.; Bilia, A.R.; Bergonzi, M.C. Nanoemulsion for improving oral bioavailability of *Vitex agnus castus* extract: Formulation and in vitro evaluation using PAMPA and Caco-2 approaches. *Drug Deliv.* **2017**, *24*, 380–390. [[CrossRef](#)] [[PubMed](#)]
17. Porter, C.J.; Wasan, K.M.; Constantinides, P. Lipid-based systems for the enhanced delivery of poorly water soluble drugs. *Adv. Drug Deliv. Rev.* **2008**, *60*, 615–616. [[CrossRef](#)] [[PubMed](#)]
18. Chakraborty, S.; Shukla, D.; Mishra, B.; Singh, S. Lipid-an emerging platform for oral delivery of drugs with poor bioavailability. *Eur. J. Pharm. Biopharm.* **2009**, *73*, 1–15. [[CrossRef](#)] [[PubMed](#)]
19. Jia, L. Nanoparticle formulation increases oral bioavailability of poorly soluble drugs: Approaches experimental evidences and theory. *Curr. Nanosci.* **2005**, *1*, 237–243. [[CrossRef](#)] [[PubMed](#)]
20. Pouton, C. Formulation of poorly water-soluble drugs for oral administration: Physicochemical and physiological issues and the lipid formulation classification system. *Eur. J. Pharm. Sci.* **2006**, *29*, 278–287. [[CrossRef](#)] [[PubMed](#)]
21. Beloqui Garcia, A.; Solinís, M.A.; Rodríguez-Gascón, A.; Almeida, A.J.; Préat, V. Nanostructured lipid carriers: Promising drug delivery systems for future clinics. *Nanomedicine* **2016**, *12*, 143–161. [[CrossRef](#)] [[PubMed](#)]
22. USA FDA IIG. Available online: www.fda.gov/Food/IngredientsPackagingLabeling/GRAS/SCOGS/default.htm (accessed on 22 June 2018).
23. Strickley, R. Solubilizing excipients in oral and injectable formulations. *Pharm Res.* **2004**, *21*, 201–230. [[CrossRef](#)] [[PubMed](#)]
24. Nanjwade, B.K.; Patel, D.J.; Udhani, R.A.; Manvi, F.V. Functions of lipids for enhancement of oral bioavailability of poorly water-soluble drugs. *Sci. Pharm.* **2011**, *79*, 705–727. [[CrossRef](#)] [[PubMed](#)]
25. Müller, R.H. Solid lipid nanoparticles (SLN) for controlled drug delivery—a review of the state of the art. *Eur. J. Pharm. Biopharm.* **2000**, *50*, 161–177. [[CrossRef](#)]
26. Hoh, C.S.; Boocock, D.J.; Marczylo, T.H.; Brown, V.A.; Cai, H. Quantitation of Silibinin, a Putative Cancer Chemopreventive Agent Derived from Milk Thistle (*Silybum marianum*), in Human Plasma by High-Performance Liquid Chromatography and Identification of Possible Metabolites. *J. Agric. Food Chem.* **2007**, *55*, 2532–2535. [[CrossRef](#)] [[PubMed](#)]
27. Kvasnicka, F.; Biba, B.; Sevcik, R.; Voldrich, M.; Kratka, J. Analysis of the active components of silymarin. *J. Chromatogr. A* **2003**, *990*, 239–245. [[CrossRef](#)]

28. Voroneanu, L.; Nistor, I.; Dumea, R.; Apetrii, M.; Covic, A. Analysis of Randomized Controlled Trials. *J. Diabetes Res.* **2016**, *2016*, 5147468. [[CrossRef](#)] [[PubMed](#)]
29. Huseini, H.F.; Larijani, B.; Heshmat, R.; Fakhrzadeh, H.; Radjabipour, B. The efficacy of *Silybum marianum* (L.) Gaertn. (Silymarin) in the treatment of type II diabetes: A randomized, double-blind, placebo-controlled, clinical trial. *Phytother. Res.* **2006**, *20*, 1036–1039. [[CrossRef](#)] [[PubMed](#)]
30. Guigas, B.; Naboulsi, R.; Villanueva, G.R.; Taleux, N.; Lopez-Novoa, J.M. The Flavonoid Silibinin Decreases Glucose-6-Phosphate Hydrolysis in Perfused Rat Hepatocytes by an Inhibitory Effect on Glucose-6-Phosphatase. *Cell Physiol. Biochem.* **2007**, *20*, 925–934. [[CrossRef](#)] [[PubMed](#)]
31. Zhang, J.Q.; Liu, J.; Li, X.L.; Jasti, B.R. Preparation and characterization of solid lipid nanoparticles containing silibinin. *Drug Deliv.* **2007**, *14*, 381–387. [[CrossRef](#)] [[PubMed](#)]
32. Schwarz, C.; Mehnert, W. Freeze-drying of drug-free and drug-loaded solid lipid nanoparticles. *Int. J. Pharm.* **1997**, *157*, 171–179. [[CrossRef](#)]
33. Righeschi, C.; Coronello, M.; Mastrantonio, A.; Isacchi, B.; Bergonzi, M.C.; Mini, E.; Bilia, A.R. Strategy to provide a useful solution to effective delivery of dihydroartemisinin: Development, characterization and in vitro studies of liposomal formulations. *Colloids Surf. B* **2014**, *116*, 121–127. [[CrossRef](#)] [[PubMed](#)]
34. Bergonzi, M.C.; Hamdouch, R.; Mazzacupa, F.; Isacchi, B.; Bilia, A.R. Optimization, characterization and in vitro evaluation of curcumin microemulsions. *LWT-Food Sci. Technol.* **2014**, *59*, 148–155. [[CrossRef](#)]
35. Wohnsland, F.; Faller, B. High-throughput permeability pH profile and high-throughput alkane/water log P with artificial membranes. *J. Med. Chem.* **2001**, *44*, 923–930. [[CrossRef](#)] [[PubMed](#)]
36. Sugano, K.; Hamada, H.; Machida, M.; Ushio, H. High throughput prediction of oral absorption: Improvement of the composition of the lipid solution used in parallel artificial membrane permeation assay. *J. Biomol. Screen.* **2001**, *6*, 189–196. [[CrossRef](#)] [[PubMed](#)]
37. Bigagli, E.; Cinci, L.; D'Ambrosio, M.; Luceri, C. Pharmacological activities of an eye drop containing *Matricaria chamomilla* and *Euphrasia officinalis* extracts in UVB-induced oxidative stress and inflammation of human corneal cells. *J. Photochem. Photobiol. B* **2017**, *173*, 618–625. [[CrossRef](#)] [[PubMed](#)]
38. Mehnert, W.; Mäder, K. Solid lipid nanoparticles: Production, characterization and applications. *Adv. Drug Deliv. Rev.* **2012**, *64*, 83–101. [[CrossRef](#)]
39. Wang, T.; Xue, J.; Hu, Q.; Zhou, M.; Luo, Y. Preparation of lipid nanoparticles with high loading capacity and exceptional gastrointestinal stability for potential oral delivery applications. *J. Colloid Interface Sci.* **2017**, *507*, 119–130. [[CrossRef](#)] [[PubMed](#)]
40. Khan, S.; Baboota, S.; Ali, J.; Narang, R.S.; Narang, J.K. Nanostructured lipid carriers: An emerging platform for improving oral bioavailability of lipophilic drugs. *Int. J. Pharm. Investig.* **2015**, *5*, 182–191. [[CrossRef](#)] [[PubMed](#)]
41. Luo, Y.; Teng, Z.; Li, Y.; Wang, Q. Solid lipid nanoparticles for oral drug delivery: Chitosan coating improves stability, controlled delivery, mucoadhesion and cellular uptake. *Carbohydr. Polym.* **2015**, *122*, 221–229. [[CrossRef](#)] [[PubMed](#)]
42. Jia, L.J.; Zhang, D.R.; Li, Z.Y.; Feng, F.F.; Wang, Y.C.; Dai, W.T.; Duan, C.X.; Zhang, Q. Preparation and characterization of silybin-loaded nanostructured lipid carriers. *Drug Deliv.* **2010**, *17*, 11–18. [[CrossRef](#)] [[PubMed](#)]
43. Kansy, M.; Senner, F.; Gubernator, K. Physicochemical high throughput screening: Parallel artificial membrane permeation assay in the description of passive absorption processes. *J. Med. Chem.* **1998**, *41*, 1007–1010. [[CrossRef](#)] [[PubMed](#)]
44. Petit, C.; Bujard, A.; Skalicka-Wozniak, K.; Cretton, S.; Houriet, J.; Christen, P.; Carrupt, P.A.; Wolfender, J.L. Prediction of the passive intestinal absorption of medicinal plant extract constituents with the Parallel Artificial Membrane Permeability Assay (PAMPA). *Planta Med.* **2016**, *82*, 424–431. [[CrossRef](#)] [[PubMed](#)]
45. Patrick, J.W.; Gamez, R.C.; Russell, D.H. The Influence of Lipid Bilayer Physicochemical Properties on Gramicidin a Conformer Preferences. *Biophys. J.* **2016**, *110*, 1826–1835. [[CrossRef](#)] [[PubMed](#)]

